BRAIN CONNECTIVITY
Volume 7, Number 1, 2017

DOI: 10.1089/brain.2015.0406

Contrasting Effects of Posttraumatic Stress Disorder and Mild Traumatic Brain Injury on the Whole-Brain Resting-State Network: A Magnetoencephalography Study

Jared A. Rowland,[1–3] Jennifer R. Stapleton-Kotloski,[1,4] Greg E. Alberto,[2] Justin A. Rawley,[5] Robert J. Kotloski,[6,7] Katherine H. Taber,[1,8,9] and Dwayne W. Godwin[2]

Abstract

The aim of this study was to evaluate alterations in whole-brain resting-state networks associated with posttraumatic stress disorder (PTSD) and mild traumatic brain injury (mTBI). Networks were constructed from locations of peak statistical power on an individual basis from magnetoencephalography (MEG) source series data by applying the weighted phase lag index and surrogate data thresholding procedures. Networks representing activity in the alpha bandwidth as well as wideband activity (DC-80 Hz) were created. Statistical comparisons were adjusted for age and education level. Alpha network results demonstrate reductions in network structure associated with PTSD, but no differences associated with mTBI. Wideband network results demonstrate a shift in connectivity from the alpha to theta bandwidth in both PTSD and mTBI. Also, contrasting alterations in network structure are noted, with increased randomness associated with PTSD and increased structure associated with mTBI. These results demonstrate the potential of the analysis of MEG resting-state networks to differentiate two highly comorbid conditions. The importance of the alpha bandwidth to resting-state connectivity is also highlighted, while demonstrating the necessity of considering activity in other bandwidths during network construction.

Keywords: brain networks; graph theory; magnetoencephalography; posttraumatic stress disorder; traumatic brain injury

Introduction

Posttraumatic stress disorder (PTSD) and traumatic brain injury (TBI) are common conditions in the civilian as well as military and veteran populations. Mild TBI (mTBI) is commonly associated with small, diffuse heterogeneous alterations in brain structure and function (Niogi and Mukherjee, 2010). In contrast, functional neuroimaging studies and meta-analyses have consistently demonstrated altered activity in specific areas (i.e., the amygdala, hippocampus, insula, anterior cingulate cortex, and medial prefrontal cortex) in individuals with PTSD (Etkin and Wager, 2007; Hayes et al., 2012; Hughes and Shin, 2011; Patel et al., 2012). Graph theory-based network analysis provides new ways to explore and understand relationships between and among brain regions (Bullmore and Sporns, 2009; Stam and van Straaten, 2012). Network analysis may be able to provide unique information regarding alterations in neurobiological function not possible using analyses focused on a single brain site or the relationship between a pair of sites. The aim of this study was to investigate how a history of mTBI and/or a diagnosis of PTSD may alter the whole-brain resting-state network in postdeployment veterans.

Two recent studies have applied graph-based network analysis to the study of PTSD. Lei and associates (2015) compared Chinese civilians ~1 year following an earthquake using functional magnetic resonance imaging (fMRI). Overall, PTSD was associated with higher values of clustering coefficient,

[1]Research and Academic Affairs Service Line, Mid Atlantic Mental Illness Research Education and Clinical Center, W.G. (Bill) Hefner VA Medical Center, Salisbury, North Carolina.
Departments of [2]Neurobiology and Anatomy, [3]Psychiatry and Behavioral Medicine, [4]Neurology, and [5]Radiation Oncology, Wake Forest School of Medicine, Winston-Salem, North Carolina.
[6]Department of Neurology, University of Wisconsin School of Medicine and Public Health, Madison, Wisconsin.
[7]Department of Neurology, William S. Middleton VA Medical Center, Madison, Wisconsin.
[8]Division of Biomedical Sciences, Edward Via College of Osteopathic Medicine, Blacksburg, Virginia.
[9]Department of Physical Medicine and Rehabilitation, Baylor College of Medicine, Houston, Texas.

global efficiency, and local efficiency, as well as lower values of characteristic path length, but this did not result in a significant difference in small-worldness. In contrast, when the authors applied the network-based statistic (NBS) approach (Zalesky et al., 2010), a subnetwork was identified in which connectivity was significantly reduced for participants with PTSD. Dunkley and associates (2014) examined combat exposed soldiers with and without PTSD by applying NBS to resting-state magnetoencephalography (MEG). The authors identified a subnetwork in the high gamma bandwidth located primarily in the left hemisphere with increased connectivity in participants with PTSD. In addition to network analysis, several studies have examined differences in resting-state functional connectivity between individuals with and without PTSD. These studies have demonstrated reductions in functional connectivity associated with PTSD using both MEG and fMRI (Bluhm et al., 2009; Engdahl et al., 2010; Georgopoulos et al., 2010; James et al., 2012; Lanius et al., 2010a; Sripada et al., 2012; Zhou et al., 2012). Overall, findings are mixed regarding the effect of PTSD on the resting-state network. This ambiguity likely reflects differences in analytic methods and sample characteristics. The most consistent finding is reduced functional connectivity associated with PTSD; however, these studies did not examine how this reduction is related to network metrics.

Only two studies have applied graph theory-based network analysis to characterize whole-brain resting-state in participants with mTBI alone, both using fMRI. Messe and associates (2013) found reductions in modularity 6 months postinjury in participants with mTBI who developed postconcussive syndrome (PCS). Conversely, Han and associates (2014) found an increase in modularity in participants with mTBI scanned within 90 days of injury that returned to baseline at follow-up between 6 and 12 months. Studies evaluating resting-state functional connectivity, but not applying network analysis, have also produced mixed findings. Several studies have reported increased connectivity in frontal regions paired with decreased connectivity in posterior regions related to the default mode network (DMN; Iraji et al., 2015; Mayer et al., 2011; Palacios et al., 2013; Zhou et al., 2012). Using MEG, Tarapore and associates (2013) found an increased percentage of disconnected voxels in participants with TBI, which was significantly reduced at a 2-year follow-up in a subset of the sample. These findings suggest that mTBI may have complex effects on brain connectivity, possibly mediated by anatomic location, time since injury, and outcome metric.

A single study has examined network metrics in a cohort of postdeployment veterans with both PTSD and mTBI history (Spielberg et al., 2015). No main effects of PTSD severity or presence of mTBI were identified. However, NBS revealed that increased symptoms of re-experiencing were associated with lower connectivity in a subnetwork involving the right hippocampus, posterior cingulate, and prefrontal regions. A second subnetwork was identified that showed reduced connectivity related to symptoms of re-experiencing only in the presence of comorbid mTBI involving the caudate, putamen, and insula.

As a whole, the literature examining whole-brain resting-state networks in individuals with PTSD and mTBI history has produced varied results. Overall, PTSD is generally associated with broad reductions in functional connectivity, although this does not always result in between-group differences in network metrics. Studies investigating mTBI have also generally produced mixed results, likely related to the heterogeneity in injury characteristics and symptom presentation following mTBI. Studies involving veteran samples have most commonly reported reductions in functional connectivity occurring with each of these conditions that have been related to symptom severity.

The current study compares whole-brain resting-state network metrics between postdeployment veterans with PTSD-only, with mTBI-only, with both PTSD and mTBI, as well as healthy control postdeployment veterans without psychiatric diagnosis or TBI history. Based on the results of studies utilizing postdeployment veterans and the common finding of reduced functional connectivity, we hypothesized that the brain networks of participants with PTSD would have an increased resemblance to random networks (e.g., reduced clustering coefficient, increased average path length, and reduced small-worldness). Similarly, we hypothesized that mTBI history would also be associated with an increased resemblance to random networks rather than increased connectivity or network structure since participants are in the chronic state with exclusions for injuries of severity greater than mild. Finally, we hypothesized that the presence of both PTSD and mTBI history comorbidly would have a summative effect on network metrics, further pushing the network toward randomness.

Materials and Methods

This project was reviewed and approved by the institutional review board at the W.G. (Bill) Hefner VA Medical Center in Salisbury, North Carolina. The welfare and privacy of human subjects were protected. Each participant voluntarily provided verbal and written informed consent before any study activities.

Participants

Participants included 28 veterans, 6 diagnosed with PTSD-only, 6 diagnosed with mTBI-only, 6 diagnosed with both PTSD and mTBI, and 10 healthy control participants without Axis I diagnosis. Two participants diagnosed with both PTSD and mTBI were additionally diagnosed with depression. No other comorbid psychiatric diagnoses were present in the sample. Inclusion criteria included (1) Operation Enduring Freedom/Operation Iraqi Freedom/Operation New Dawn (OEF/OIF/OND) postdeployment veteran, (2) male, (3) right handed, (4) 18 years of age or older, and (5) able to tolerate enclosed space for MRI. Exclusion criteria included (1) presence of ferrous metal or implanted devices incompatible with MRI, (2) use of anticonvulsants, benzodiazepines, gamma-aminobutyric acid (GABA) agonists, or narcotic medications, (3) presence of neurological disorder other than mTBI (e.g., stroke, seizure). Control participants were matched for age and education. Average age of participants was 39.0 (SD = 9.5) years, participants had completed an average of 13.7 (SD = 1.2) years of education, and were 58% Caucasian. Average time since trauma in individuals with PTSD was 6.4 years (SD = 1.9). Average time since injury for individuals with mTBI history was 6.2 years (SD = 2.7).

Participants continued treatment as usual, including the use of common psychiatric medications (e.g., selective serotonin

reuptake inhibitors, norepinephrine dopamine reuptake inhibitors, serotonin agonists). Five participants with PTSD-only, one participant with mTBI-only, three participants with both PTSD and mTBI, and no control participants reported taking psychiatric medications. Previous studies including participants with PTSD being treated with psychiatric medications have not found differences in brain activity associated with medication status (Bluhm et al., 2009; Chen and Etkin, 2013; Lanius et al., 2010b).

Diagnosis and symptom report

The Structured Clinical Interview for DSM-IV Diagnosis (SCID; First et al., 1996) was used to determine the presence or absence of any Axis I psychiatric diagnosis. The SCID is a structured clinician-administered interview considered the gold standard for psychiatric diagnosis. A separate clinician administered interview was used to determine the presence or absence of mTBI history across the lifespan according to the American Congress of Rehabilitation Medicine criteria (Menon et al., 2010).

Participants were administered the PTSD Checklist–Military version (PCL-M; Weathers et al., 1993) and the Rivermead Postconcussive Symptoms Questionnaire (RPSQ; King et al., 1995) immediately before neuroimaging. The PCL-M is a self-report questionnaire evaluating the 17 DSM-IV symptoms of PTSD on a Likert scale from 1 ''Not at all'' to 5 ''Extremely'' with subscales corresponding to the B, C, and D criteria as outlined in the DSM-IV (American Psychiatric Association, 2000). The RPSQ is a self-report questionnaire evaluating common postconcussive symptoms. The administration was modified because not all participants had mTBI history. Participants compared the experience of listed symptoms at the present time with the experience of listed symptoms before any deployments, rather than before injury. This modification will capture the pre/post changes due to mTBI in those with an injury and control for the effects of time and deployment in those without mTBI history.

MEG recordings

Data were acquired using a whole-head CTF Systems, Inc., MEG 2005 neuromagnetometer system equipped with 275 first-order axial gradiometer coils housed within a magnetically shielded room. Head localization was achieved using a conventional three-point fiducial system (nasion and preauricular points). Recording was conducted with the participant seated upright with eyes open for 8 min. Data were sampled at 600 Hz over a DC-150 Hz bandwidth. MEG data were preprocessed using synthetic third-order gradient balancing, whole trial DC offset, and band pass filtered from DC-80 Hz with a 60 Hz notch filter. Data were visually inspected for obvious muscle artifact, and such epochs were discarded from further analyses. Following MEG recording, a T1 weighted MRI scan was obtained for each participant for the purpose of localizing MEG signals.

Network analysis

The approach to network creation used in this analysis avoided *a priori* assumptions regarding areas of the brain active at rest and did not rely on identifying regions of interest. Instead, a well-validated beamformer (synthetic aperture magnetometry [SAM]) (Hillebrand et al., 2005; Robinson and Vrba, 1998) was used to identify areas of peak activity in the brain for each individual. These areas were used as the nodes of the network, creating a unique network for each individual representing whole-brain resting-state activity (section Node Identification below). Time series data of brain activity at each node was then extracted (source series) and used for calculating functional connectivity (section Estimating Functional Connectivity Between Nodes below). For the primary analysis, connectivity was examined within the alpha bandwidth, as this frequency range is primarily associated with resting-state brain activity. Networks were then thresholded (section Thresholding below) and binarized for the calculation of network metrics (section Calculation of Network Metrics below).

Node identification. SAM was applied (voxel size of 5 mm^3, lead fields for equivalent current dipoles, maximizing noise-normalized power) using a three spherical shell, multiple local spheres head model (Huang et al., 1999) to construct noise-normalized statistical parametric maps identifying areas of significant brain activity. Brain regions may be active across different regions of the frequency spectrum; therefore, SAM was applied in several frequency ranges [delta (0.5–4 Hz), theta (4–8 Hz), alpha (8–13 Hz), beta (13–30 Hz), gamma (30–80 Hz), as well as DC-80 Hz] to maximize the likelihood active brain regions were identified. For each individual, brain regions identified as significantly active in any frequency range were included as nodes in that individual's network.

Next, source series were calculated for each node, representing the unique weighted sum of the output across all MEG sensors for a specific location in the brain (Hillebrand et al., 2005; Robinson et al., 2002). Source series retain the same temporal resolution and frequency characteristics as the MEG sensor data and have been used in numerous studies to investigate brain activity both at rest and using event-related paradigms (Beal et al., 2010; Cheyne et al., 2007; Cornwell et al., 2008, 2012; Douw et al., 2013; Hillebrand et al., 2012; Hung et al., 2010, 2012; Luo et al., 2007, 2013; Moses et al., 2009; Quraan et al., 2011; Riggs et al., 2009; Stapleton-Kotloski et al., 2014).

Estimating functional connectivity between nodes. The weighted phase lag index (wPLI; Vinck et al., 2011) was calculated between all pairs of source series to measure functional connectivity between nodes. The wPLI is a frequency domain measure of connectivity less sensitive to spurious volume conduction as demonstrated by Vinck and associates (2011). The wPLI measures the consistency of phase difference (range 0–1) between two sources, with values closer to 1 indicating a stronger connectivity. The wPLI was adapted to resting-state data by dividing the initial 4 min of the resting-state scan into 6 sec, nonoverlapping epochs. The cross-spectrum within each epoch was calculated using Welch's method as implemented in Matlab 2014a and these cross-spectra were used to calculate the wPLI. Connectivity was operationalized as the highest wPLI value occurring in the alpha bandwidth (8–13 Hz). An exploratory analysis was conducted operationalizing connectivity as the highest wPLI value between 0.5 and 80 Hz (wideband).

Thresholding. Empirical evidence suggests that the use of surrogate data reduces false-positive identification of connections between nodes in comparison with other thresholding techniques (Toppi et al., 2012). Surrogate data were calculated following the suggestions of Prichard and Theiler (1994) using a Fourier transform to randomize the phase of the data while maintaining the power spectrum. The wPLI values of 10,000 unique pairs of surrogate time series were calculated for each participant. Connectivity between each node pair was compared to the surrogate value at the identical frequency bin (i.e., 10.25 or 8.75 Hz) and retained if at least two standard deviations higher. The resulting networks were then thresholded following the methods of Hayasaka and Laurienti (2010) using the equation $S = \log(N)/\log(K)$, where N represents the number of nodes in the network and K the average degree. We selected $S = 2.5$ as prior research has demonstrated equivalence of S values between 2 and 4 (Hayasaka and Laurienti, 2010). Since N and S are static values for a given participant, we removed the weakest connections from the network until the equation was satisfied. The average connection strength of the resulting network was calculated (*wPLI Mean*) and the network was binarized.

Calculation of network metrics. Network metrics calculated for the alpha network are listed in Table 2, while metrics calculated for the wideband network are listed in Table 3. Unless otherwise stated, metrics were calculated using definitions provided in Stam and Reijneveld (2007). *Small World* was calculated as defined in Watts and Strogatz (1998). The average of the clustering coefficient and path length of 500 independently generated random networks with the same number of nodes and degree distribution as the original network were used for the calculation of Small World. *K-core value* was calculated as defined in Seidman (1983). The maximum K-core value of the network (*K-Core Degree*) and the number of nodes present at the K-Core Degree (*K-Core Nodes*) were calculated for each network. *Rich Club* was calculated as defined in Colizza and associates (2006). The average Rich Club Coefficient of 500 independently generated random networks was used for this calculation. The *Rich Club Peak* is the peak value of the Rich Club Coefficient, *Rich Club Degree* is the degree of the Rich Club Peak, and *Rich Club Nodes* is the number of nodes present at Rich Club Degree. The Rich Club phenomenon was measured by subtracting the Rich Club Coefficient at Degree = 1 from the Rich Club Peak (*Rich Club Diff*).

Modularity was calculated as defined in Blondel and associates (2008). The Louvain method of community detection was used. Following the recommendations of the Brain Connectivity Toolbox, the analysis was run 500 times, using the average Q and average number of modules (*Number Modules*) as outcome variables.

Since networks were created individually for each participant, the number of nodes within each network (*Nodes*) varied, ranging from 83 to 179. To control for possible effects of network size, each network metric was normalized by the number of nodes in the network from which it was calculated.

The structure of the wideband network allows for the calculation of additional metrics since connections may occur across all frequencies. For example, it is possible to calculate the percentage of connections occurring within each bandwidth (*Delta Connections*, *Theta Connections*, *Alpha Connections*, *Beta Connections*, *Gamma Connections*) as well as the mode frequency of connectivity (*Mode Connect*).

Materials

Beamforming and source series construction were completed using software provided by MISL (MEG International Services Ltd., Coquitlam, BC, Canada). Further analyses of source series data and network creation were conducted using Matlab 2014a. Network metrics were calculated using the Brain Connectivity Toolbox (Rubinov and Sporns, 2010), as well as functions created by members of the study team. Statistical analyses were conducted using IBM SPSS Statistics Version 21.

Analyses

Between-group differences in continuous demographic variables were examined using 2 (yes/no PTSD) × 2 (yes/no mTBI) univariate ANOVAs. Differences in categorical demographic variables were examined with chi-square analyses. Between-group differences in normalized network metrics were examined using 2 (yes/no PTSD) × 2 (yes/no mTBI) univariate ANCOVAs controlling for age and years of education. Bivariate correlations were used to examine the linear relationship between normalized network metrics with PTSD and postconcussive symptoms. Results are presented using an uncorrected alpha level of 0.05 along with effect sizes (partial eta-squared and Cohen's d) to aid interpretation, as no result remained significant after applying a false discovery rate correction.

Results

Demographics

See Table 1 for means and standard deviations of demographic variables. There were no significant between-group differences in age or education. There was a significant interaction between PTSD and mTBI for number of deployments ($F(1,24) = 7.41$, $p < 0.02$, partial eta-squared = 0.236), demonstrating that individuals with mTBI but without PTSD had a significantly higher number of deployments than other participants. A higher proportion of participants with PTSD identified as a racial minority, $\chi^2_1 = 7.00$, $p < 0.02$. There was a significant main effect of PTSD for the PCL-M total ($F(1,24) = 28.41$, $p < 0.001$, partial eta-squared = 0.542), cluster B ($F(1,24) = 25.71$, $p < 0.001$, partial eta-squared = 0.517), cluster C ($F(1,24) = 21.6$, $p < 0.001$, partial eta-squared = 0.474), cluster D ($F(1,24) = 26.31$, $p < 0.001$, partial eta-squared = 0.523), and RPSQ Total ($F(1,24) = 26.98$, $p < 0.001$, partial eta-squared = 0.529), each indicating participants with PTSD scored higher than those without.

Alpha network outcomes

Means and standard deviations of alpha network metrics can be seen in Table 2. There was a significant interaction between PTSD and mTBI for clustering coefficient ($F(1,22) = 5.482$, $p < 0.029$, partial eta squared = 0.199, Cohen's $d = 0.66$). *Post hoc* group comparisons suggest that individuals with PTSD-only had significantly lower clustering coefficient than

Table 1. Mean (Standard Deviation) of Demographic Variables, Unless Otherwise Noted

	No PTSD diagnosis		*PTSD diagnosis*					
Variable	*No TBI history* (n = *10*)	*TBI history* (n = *6*)	*No TBI history* (n = *6*)	*TBI history* (n = *6*)	*No PTSD total* (n = *16*)	*PTSD total* (n = *12*)	*TBI total* (n = *12*)	*No TBI total* (n = *16*)
Age	38.1 (10.7)	35.3 (12.6)	43.3 (9.8)	33.5 (5.9)	37.1 (11.1)	38.4 (9.3)	34.4 (9.4)	40.1 (10.4)
Education	14.0 (2.1)	14.0 (1.8)	13.0 (0.9)	12.8 (1.0)	14.0 (1.9)	12.9 (0.9)	13.4 (1.5)	13.6 (1.7)
Deployments[a–c]	1.5 (0.5)	3.2 (1.5)	1.2 (0.4)	1.2 (0.4)	2.1 (1.3)	1.2 (0.4)	2.2 (1.5)	1.4 (0.5)
PCL-M B[a]	5.5 (0.5)	7.8 (2.4)	12.5 (3.7)	15.2 (6.6)	6.4 (1.9)	13.8 (5.3)	11.5 (6.1)	8.1 (4.1)
PCL-M C[a]	7.2 (0.4)	12.5 (4.3)	19.5 (5.1)	19.3 (9.5)	9.2 (3.7)	19.4 (7.3)	15.9 (7.9)	11.8 (6.8)
PCL-M D[a]	6.5 (2.0)	9.3 (4.0)	17.8 (5.0)	15.8 (6.9)	7.6 (3.1)	16.8 (5.9)	12.6 (6.4)	10.8 (6.6)
PCL-M total[a]	19.2 (2.6)	29.7 (10.0)	49.8 (12.5)	50.3 (21.7)	23.1 (8.1)	50.1 (16.9)	40.0 (19.4)	30.7 (17.1)
RPSQ total[a]	11.7 (7.4)	16.0 (9.3)	36.5 (8.2)	31.2 (14.9)	13.3 (8.1)	33.8 (11.8)	23.6 (14.2)	21.0 (14.5)
Minority status (% positive)[a]	10	0	50	50	6		25	25

$n = 28$.
[a]PTSD main effect $p < 0.05$.
[b]TBI main effect $p < 0.05$.
[c]PTSD-TBI interaction $p < 0.05$.
PCL-M, PTSD Checklist–Military version; PTSD, posttraumatic stress disorder; RPSQ, Rivermead Postconcussive Symptoms Questionnaire; TBI, traumatic brain injury.

participants with mTBI-only ($F(1,8) = 7.926$, $p < 0.023$, partial eta squared = 0.498) and marginally lower than control participants ($F(1,12) = 4.168$, $p < 0.064$, partial eta squared = 0.258) but were not different from participants with both PTSD and mTBI. Other subgroup comparisons were not significant. A significant interaction was found between PTSD and mTBI for Small World ($F(1,22) = 5.048$, $p < 0.035$, partial eta squared = 0.187, Cohen's $d = 0.86$; Fig. 1A). *Post hoc* comparisons suggest that participants with PTSD-only displayed significantly lower values of Small World than participants with mTBI-only ($F(1,8) = 8.475$, $p < 0.02$, partial eta squared = 0.514) and marginally lower values than participants with PTSD and mTBI ($F(1,8) = 5.08$, $p < 0.054$, partial eta squared = 0.388) and control participants ($F(1,12) = 4.105$, $p < 0.066$, partial eta squared = 0.255). Small World was above 1 for all but two participants, each in the PTSD-only group. There was a significant interaction between PTSD and mTBI for the number of modules present ($F(1,22) = 7.186$, $p < 0.014$, partial eta squared = 0.246, Cohen's $d = 0.65$). *Post hoc* comparisons did not reveal significant between-group differences. Qualitatively, participants with mTBI-only and with PTSD-only had fewer modules present. There were no other significant between-group differences in normalized global network metrics. Correlations between the PCL-M total score, RPSQ total score, and normalized global network metrics were not significant.

Wideband network outcomes

Means and standard deviations of wideband network metrics can be seen in Table 3. There was a significant main effect of PTSD for Small World ($F(1,22) = 6.13$, $p < 0.021$, partial eta-squared = 0.218, Cohen's $d = 0.53$), suggesting that networks of participants with PTSD displayed *lower* levels of small-worldness (Fig. 1B). There was also a significant main effect of mTBI ($F(1,22) = 7.31$, $p < 0.013$, partial eta-squared = 0.249, Cohen's $d = 0.65$) for Small World, suggesting that networks of participants with mTBI history displayed *higher* levels of small-worldness. There were no significant differences for other measured network metrics. Examination of effect sizes suggests that the difference in Small World is primarily related to differences in clustering coefficient (PTSD, $F(1,22) = 3.06$, $p < 0.094$, partial eta-squared = 0.122, Cohens' $d = 0.33$; mTBI, $F(1,22) = 4.04$, $p < 0.057$, partial eta-squared = 0.155, Cohen's $d = 0.53$) rather than path length (PTSD, $F(1,22) = 0.01$, $p < 0.939$, partial eta squared = 0.000, Cohen's $d = 0.25$; mTBI, $F(1,22) = 1.42$, $p < 0.246$, partial eta squared = 0.061, Cohen's $d = 0.41$). Similar to the alpha network, Small World was above 1 for all but two participants, each in the PTSD-only group, one of which also had Small World below 1 in the alpha network. Correlations between network metrics and symptom report were not significant. Modal connectivity occurred in the alpha bandwidth for all but four participants (two control, one PTSD-only, one mTBI-only) and was not different between groups. An average of 42.4% (SD = 0.21) of connectivity occurred within the alpha band. The percentage of connectivity was not significantly different between groups within the delta, alpha, beta, or gamma bandwidths; however, there was a significant interaction for Theta Connections ($F(1,22) = 8.66$, $p < 0.008$, partial eta squared = 0.282, Cohen's $d = 0.34$; Fig. 2). *Post hoc* comparisons reveal significantly higher Theta Connections in the mTBI-only group compared to the Control group ($F(1,12) = 11.98$, $p < 0.005$, partial eta squared = 0.500) and marginal significance comparing PTSD-only and control participants ($F(1,12) = 3.97$, $p < 0.070$, partial eta squared = 0.248). No other comparisons were significant.

Exploratory validation of results

Further analyses were conducted to explore the robustness of these findings and provide further validation of the results. The Small World metric was chosen for this purpose because differences in this variable were found for both the Alpha and Wideband networks. Figures 3–5 display the Small World data for both networks on an individual basis with group (Control, PTSD-only, mTBI-only, comorbid PTSD/mTBI) coded by symbols so that interactions can be more easily visualized. It is important to note that prior statistical analyses

Table 2. Mean (Standard Deviation) of Alpha Network Metrics

	No PTSD diagnosis		*PTSD diagnosis*					
Variable	*No TBI history (n=10)*	*TBI history (n=6)*	*No TBI history (n=6)*	*TBI history (n=6)*	*No PTSD total (n=16)*	*PTSD total (n=12)*	*TBI total (n=12)*	*No TBI total (n=16)*
Nodes	124.4 (17.1)	124.3 (36.8)	127.2 (26.7)	115.5 (16.2)	124.4 (25.0)	121.3 (21.9)	119.9 (27.5)	125.4 (20.4)
Density	7.5 (1.4)	8.3 (3.5)	7.6 (3.0)	8.4 (1.9)	7.8 (2.3)	8.0 (2.4)	8.3 (2.7)	7.5 (2.0)
Average degree	9.0 (0.7)	9.2 (1.3)	9.0 (1.0)	9.4 (0.7)	9.1 (0.9)	9.2 (0.9)	9.3 (1.0)	9.0 (0.7)
Sum degree	1112.4 (74.3)	1103.9 (164.1)	1120.0 (126.4)	1071.3 (76.7)	1109.2 (110.9)	1095.7 (102.9)	1087.6 (123.3)	1115.2 (93.0)
Clustering coefficient[a]	0.20 (0.04)	0.19 (0.07)	0.15 (0.03)	0.22 (0.05)	0.19 (0.05)	0.19 (0.05)	0.18 (0.05)	0.20 (0.06)
Path length	1.8 (0.2)	2.0 (0.6)	2.0 (0.6)	1.9 (0.3)	1.9 (0.4)	1.9 (0.4)	1.9 (0.4)	1.9 (0.4)
Diameter	4.6 (0.7)	4.5 (1.4)	4.5 (1.5)	4.4 (0.7)	4.5 (1.0)	4.4 (1.1)	4.4 (1.1)	4.5 (1.1)
Global efficiency	0.34 (0.06)	0.39 (0.13)	0.37 (0.10)	0.37 (0.05)	0.36 (0.09)	0.37 (0.07)	0.38 (0.09)	0.35 (0.07)
Small World[a]	1.2 (0.2)	1.2 (0.3)	1.0 (0.1)	1.3 (0.1)	1.2 (0.2)	1.1 (0.2)	1.2 (0.2)	1.2 (0.2)
K-Core Degree	8.1 (1.1)	7.9 (1.6)	7.0 (1.4)	7.9 (1.2)	8.0 (1.3)	7.5 (1.3)	7.9 (1.4)	7.7 (1.3)
K-Core Nodes	26.3 (9.9)	30.6 (15.3)	39.4 (13.0)	35.7 (12.7)	27.9 (11.9)	37.6 (12.4)	33.2 (13.7)	31.2 (12.6)
Rich Club Peak	1.9 (0.5)	1.8 (0.6)	1.8 (0.5)	2.0 (0.5)	1.8 (0.5)	1.9 (0.5)	1.9 (0.5)	1.8 (0.5)
Rich Club Degree	15.0 (3.4)	13.8 (2.6)	14.6 (2.6)	14.8 (3.5)	14.6 (3.1)	14.7 (2.9)	14.3 (3.0)	14.9 (3.1)
Rich Club Nodes	17.1 (7.8)	22.3 (9.1)	17.3 (7.4)	20.3 (9.2)	19.1 (8.4)	18.8 (8.1)	21.3 (8.8)	17.2 (7.4)
Rich Club Diff	0.95 (0.4)	0.90 (0.5)	0.93 (0.3)	1.0 (0.5)	0.93 (0.4)	0.97 (0.4)	0.96 (0.5)	0.95 (0.3)
Modularity (Q)	0.29 (0.05)	0.32 (0.09)	0.28 (0.05)	0.28 (0.05)	0.30 (0.07)	0.28 (0.05)	0.30 (0.07)	0.29 (0.05)
Number Modules[a]	8.0 (2.6)	6.6 (1.8)	5.9 (1.2)	9.6 (2.9)	7.5 (2.4)	7.7 (2.8)	8.1 (2.8)	7.2 (2.4)
wPLI Mean	0.75 (0.06)	0.72 (0.09)	0.70 (0.07)	0.75 (0.42)	0.74 (0.07)	0.73 (0.06)	0.73 (0.07)	0.73 (0.06)

All variables except nodes and wPLI mean have been normalized by the number of nodes in a network and are presented $\times 10^2$ for ease of reading. $n=28$.
[a]PTSD-TBI interaction $p<0.05$.
wPLI, weighted phase lag index.

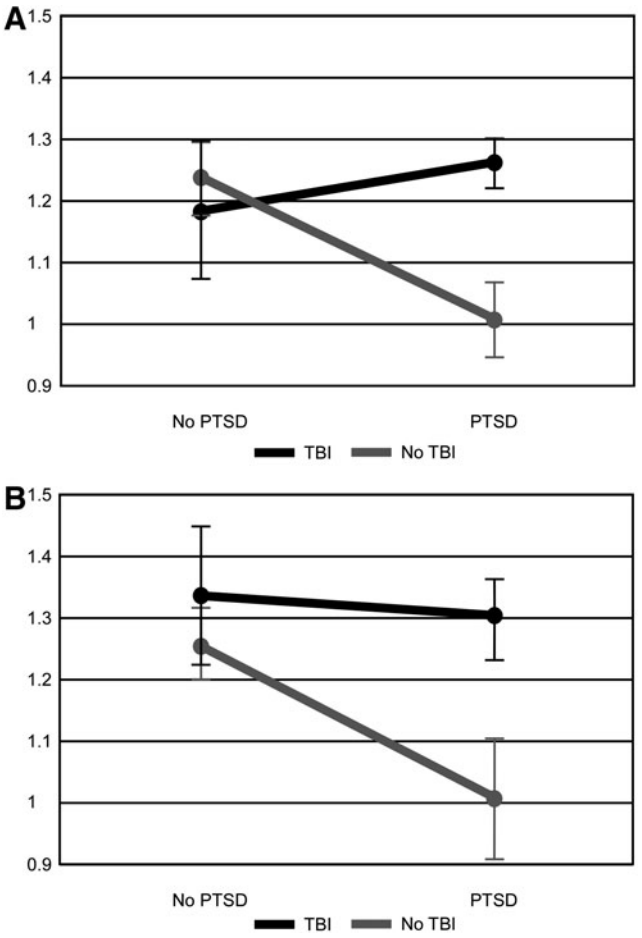

FIG. 1. Mean small worldness across groups. Error bars represent 1 standard error. **(A)** Small worldness within the alpha (8–13 Hz) network. **(B)** Small worldness within the wideband (DC-80 Hz) network. PTSD, posttraumatic stress disorder; TBI, traumatic brain injury.

included age and education as covariates, which are not reflected in the data displayed in Figures 3–5. Figure 3 displays the Small World data for each network separately. Figure 4 displays a scatter plot contrasting the Small World data from both networks. Figures 3 and 4 demonstrate significant overlap in the Small World data across groups; however, participants with PTSD-only clearly trend lower in Figure 3 and are clearly clustered in the lower left quadrant of Figure 4, visually supporting the statistical results. Participants with comorbid PTSD/mTBI history can also be seen to cluster in Figure 4, while control participants and those with mTBI-only are found throughout the range.

Cluster analysis was then used to further explore natural groupings within the data and how well those groupings represented the clinical groups. Hierarchical cluster analysis was conducted using Small World from both the Alpha and Wideband networks. Ward's method was implemented using Squared Euclidean distance. Normalization was unnecessary as the Small World variables are on the same scale. Figure 5 displays the three (Fig. 5A) and four (Fig. 5B) group solutions. Visually, the three group solution appears to capture the topography of the data best. Visual examination suggests significant heterogeneity between the clinical groupings and the results of the clustering analysis.

Discriminant analysis was then used to evaluate the results of the cluster analysis. Small World from both the Alpha and Wideband networks were evaluated first using the three group cluster and four group cluster solutions and then with the clinical groupings. Table 4 contains descriptive statistics for each model. There is little difference in performance of the three and four group solution and the clinical groupings are clearly inferior.

Discussion

The current study is the first to report a graph-based network analysis of resting-state MEG data investigating both PTSD and mTBI. The results of this study demonstrate several important findings, namely (1) PTSD, particularly in the absence of mTBI history, was associated with lower values of network metrics (reductions in clustering coefficient, modularity, and small-worldness) indicative of reduced structure and increased randomness, suggesting a shift away from local connectivity and hierarchical network structure toward larger more inclusive modules, (2) mTBI history was associated with an *increase* in small-worldness in the wideband network but was not associated with alterations in alpha network metrics, and (3) different results were observed when restricting connectivity within the alpha bandwidth, suggesting such restriction may miss important network connections occurring at other frequencies. These findings suggest that graph-based network analysis of MEG data has the potential to improve our understanding of PTSD and mTBI, and potentially to aid in the diagnosis and differentiation of these two conditions.

Findings of increased randomness in network topology associated with PTSD are consistent with those of Spielberg and associates (2015) who demonstrated decreased connectivity in specific subnetworks associated with increased symptoms of re-experiencing. The current findings are also consistent with studies associating PTSD with reduced functional connectivity of the precuneus within the DMN (Bluhm et al., 2009; Lanius et al., 2010a) and reduced connectivity, particularly in the right temporoparietal area (Engdahl et al., 2010; Georgopoulos et al., 2010).

Increased randomness in network topology may have relevance to understanding the individual clinical presentation and characteristic symptoms of individuals with PTSD. A small-world network structure minimizes the characteristic path length while maximizing the characteristic clustering coefficient, allowing highly efficient transfer of information at minimal additional wiring cost (Watts and Strogatz, 1998). A shift toward a random network (low clustering coefficient and low path length) would result in lower efficiency of information transfer and lower redundancy within the network. A reduction in modularity suggests that fewer modules are clearly present in the network and is likely related to the observed reduction in clustering coefficient. A reduction in modularity could be related to a reduction in specificity of nodes within the resting-state network and could also result in lower efficiency of information transfer in the network. These differences in network structure may be directly related to symptoms of PTSD. Reductions in network efficiency have been related to poorer cognitive performance, particularly in areas of processing speed, learning, and

Table 3. Mean (Standard Deviation) of Wideband Network Metrics, Unless Otherwise Noted

	No PTSD diagnosis		*PTSD diagnosis*					
Variable	*No TBI history* (n = *10*)	*TBI history* (n = *6*)	*No TBI history* (n = *6*)	*TBI history* (n = *6*)	*No PTSD total* (n = *16*)	*PTSD total* (n = *12*)	*TBI total* (n = *12*)	*No TBI total* (n = *16*)
Nodes	124.4 (17.1)	124.3 (36.8)	127.2 (26.7)	115.5 (16.2)	124.4 (25.0)	121.3 (21.9)	119.9 (27.5)	125.4 (20.4)
Density	7.5 (1.4)	8.3 (3.5)	7.7 (3.0)	8.4 (1.9)	7.8 (2.3)	8.0 (2.4)	8.3 (2.7)	7.5 (2.0)
Average degree	9.0 (0.6)	9.2 (1.3)	9.0 (1.1)	9.4 (0.7)	9.1 (0.9)	9.2 (0.9)	9.3 (1.0)	9.0 (0.8)
Sum degree	1112.4 (74.3)	1103.6 (164.0)	1121.6 (123.1)	1071.3 (76.7)	1109.1 (110.9)	1096.5 (101.2)	1087.4 (123.2)	1115.8 (91.6)
Clustering coefficient	0.19 (0.05)	0.21 (0.07)	0.15 (0.06)	0.21 (0.06)	0.20 (0.05)	0.18 (0.06)	0.21 (0.06)	0.18 (0.05)
Path length	1.9 (0.3)	2.0 (0.5)	1.9 (0.4)	2.1 (0.3)	1.9 (0.4)	2.0 (0.4)	2.0 (0.4)	1.9 (0.4)
Diameter	4.3 (0.9)	4.7 (1.4)	3.9 (1.2)	4.5 (0.8)	4.5 (1.1)	4.2 (1.1)	4.6 (1.1)	4.2 (1.0)
Global efficiency	0.35 (0.06)	0.38 (0.12)	0.37 (0.08)	0.40 (0.06)	0.36 (0.09)	0.38 (0.07)	0.39 (0.09)	0.36 (0.07)
Small World[a,b]	1.3 (0.2)	1.3 (0.3)	1.0 (0.2)	1.3 (0.2)	1.3 (0.2)	1.2 (0.3)	1.3 (0.2)	1.2 (0.2)
K-Core Degree	8.0 (1.4)	7.7 (1.2)	7.3 (2.4)	7.4 (1.1)	7.9 (1.3)	7.4 (1.8)	7.6 (1.1)	7.7 (1.8)
K-Core Nodes	28.6 (19.3)	30.9 (20.1)	38.0 (16.5)	39.0 (19.0)	29.4 (19.0)	38.5 (17.0)	34.9 (19.2)	32.1 (18.4)
Rich Club Peak	2.1 (0.6)	2.1 (0.7)	1.9 (0.8)	1.9 (0.4)	2.1 (0.6)	1.9 (0.6)	2.0 (0.6)	2.0 (0.7)
Rich Club Degree	16.1 (2.8)	15.4 (2.9)	15.1 (3.4)	15.8 (4.3)	15.8 (2.7)	15.4 (3.7)	15.6 (3.5)	15.7 (2.9)
Rich Club Nodes	14.3 (6.1)	16.6 (6.8)	16.4 (9.1)	17.0 (7.3)	15.1 (6.2)	16.7 (7.9)	16.8 (6.8)	15.1 (7.1)
Rich Club Diff	1.2 (0.5)	1.2 (0.6)	1.0 (0.6)	1.0 (0.3)	1.2 (0.5)	1.0 (0.5)	1.1 (0.5)	1.1 (0.6)
Modularity (Q)	0.30 (0.06)	0.31 (0.08)	0.27 (0.06)	0.31 (0.06)	0.30 (0.07)	0.29 (0.06)	0.31 (0.07)	0.29 (0.06)
Number Modules	7.4 (5.9)	7.1 (2.5)	6.3 (3.0)	5.8 (1.3)	7.3 (4.8)	6.1 (2.3)	6.5 (2.1)	7.0 (4.9)
wPLI Mean	0.81 (0.05)	0.79 (0.04)	0.77 (0.05)	0.81 (0.03)	0.80 (0.05)	0.79 (0.05)	0.80 (0.04)	0.79 (0.05)
Mode Connect	9.7 (3.9)	8.5 (3.4)	8.5 (2.4)	10.2 (1.0)	9.3 (3.7)	9.3 (2.0)	9.3 (2.6)	9.3 (3.4)
Delta Connections (%)	7.6 (7.4)	9.8 (12.9)	5.5 (8.1)	9.6 (9.5)	8.4 (9.5)	7.5 (8.7)	9.7 (10.8)	6.8 (7.5)
Theta Connections (%)[c]	4.6 (3.6)	12.3 (6.4)	14.7 (11.3)	6.1 (2.7)	7.5 (6.0)	10.4 (9.1)	9.2 (5.7)	8.4 (8.7)
Alpha Connections (%)	48.4 (24.3)	36.2 (25.8)	41.4 (20.7)	39.4 (10.4)	43.9 (24.8)	40.4 (15.6)	37.8 (18.8)	45.8 (22.6)
Beta Connections (%)	11.6 (9.0)	14.8 (6.0)	14.5 (9.1)	19.8 (9.6)	12.8 (7.9)	17.1 (9.3)	17.3 (8.1)	12.7 (8.8)
Gamma Connections (%)	27.8 (18.7)	27.0 (19.3)	24.0 (12.7)	25.1 (16.2)	27.5 (18.3)	24.6 (13.9)	26.1 (17.0)	26.4 (16.4)

All variables except nodes, wPLI mean, frequency connections, and percent connections have been normalized by the number of nodes in a network and are presented $\times 10^2$ for ease of reading. $n = 28$.
[a]PTSD main effect $p < 0.05$.
[b]TBI main effect $p < 0.05$.
[c]PTSD-TBI interaction $p < 0.05$.

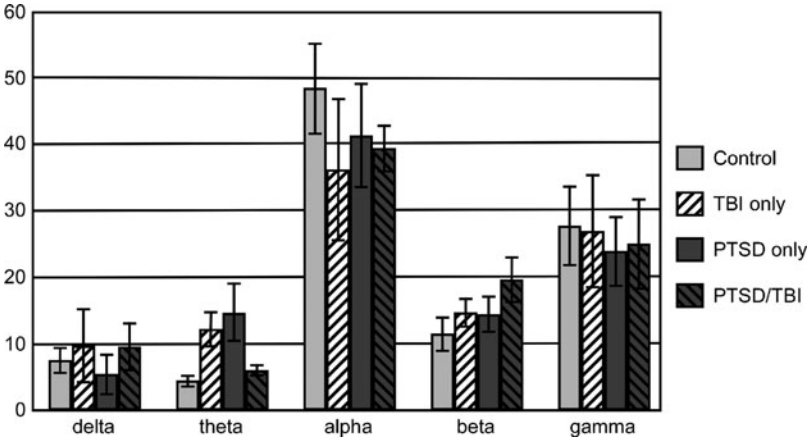

FIG. 2. Mean percentage of overall network connections occurring in each bandwidth across groups (delta: 0.5–4 Hz, theta: 4–8 Hz, alpha: 8–13 Hz, beta: 13–30 Hz, gamma: 30–80 Hz). Error bars represent 1 standard error.

memory (Bosma et al., 2009; Douw et al., 2011; Geib et al., 2015; Schedlbauer et al., 2014). Deficits in attention, learning, and memory have previously been demonstrated in individuals with PTSD (Gilbertson et al., 2006).

Networks of participants with mTBI history displayed a *greater* degree of structure and less resemblance to random networks as indicated by higher levels of clustering coefficient and small-worldness; however, individuals with mTBI history only also displayed a reduction in modularity. Of the two studies using network analysis to examine resting-state brain activity in mTBI, one found no difference after 90 days, and one found reduced modularity in those that developed PCS. The current study did not recruit based on the presence or absence of PCS, and self-report data suggest that this sample is at most mildly symptomatic. Similar results of increased connectivity (not in the context of network analysis) have been reported following moderate-to-severe TBI and, along with other differences, led to the proposal of the hyperconnectivity hypothesis (Hillary et al., 2014). However, the lack of differences in connection strength, rich-club characteristics, or degree of the k-core in the current results is contrary to this hypothesis. Reductions in modularity suggest that this increase in connectivity may not be an *improvement* to network topology, but rather a mixing of connections across modules. Unlike previous findings, this difference was not related to postconcussive symptoms in the current sample.

This is the first study to evaluate ''wideband'' connectivity using a purely phase-based metric, allowing connectivity to occur anywhere along the frequency spectrum. Using this methodology, the mode frequency of connectivity occurred in the alpha range for the majority (24/28) of individuals, confirming the importance of the alpha bandwidth in the resting state. While modal connectivity occurred in the alpha bandwidth, the majority of connections (58%) were observed *outside* this range. This is consistent with findings from studies using simultaneous electroencephalography (EEG)/fMRI to study resting-state networks demonstrating both positive (Jann et al., 2009; Knyazev et al., 2011) and negative (Laufs et al., 2003, 2006) relationships between the DMN and activity in the alpha bandwidth. A recent study by Neuner and associates (2014) demonstrated that activity in the

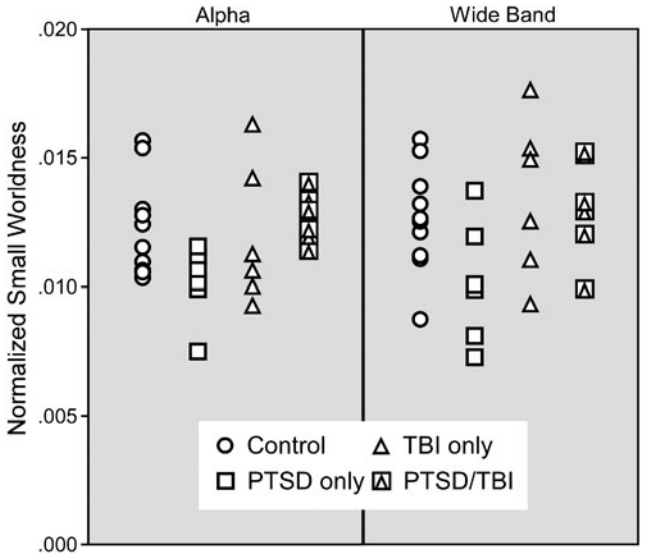

FIG. 3. Individual data for normalized small worldness presented by clinical diagnosis from the alpha (left panel) and wideband (right panel) networks.

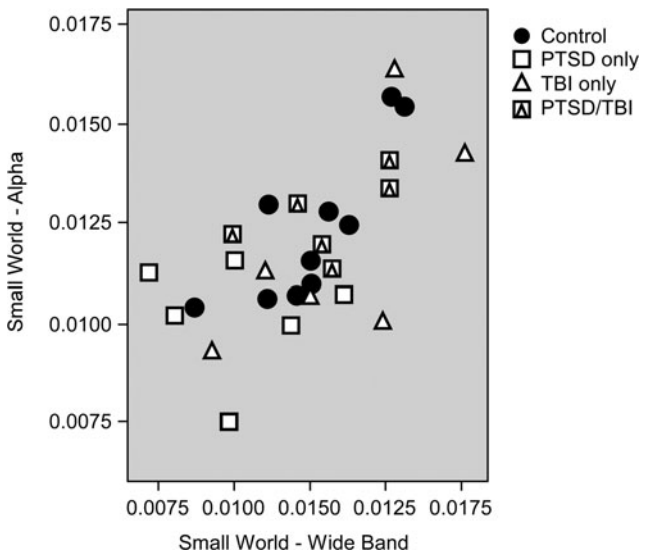

FIG. 4. Scatter plot of small worldness from the alpha network against small worldness from the wideband network.

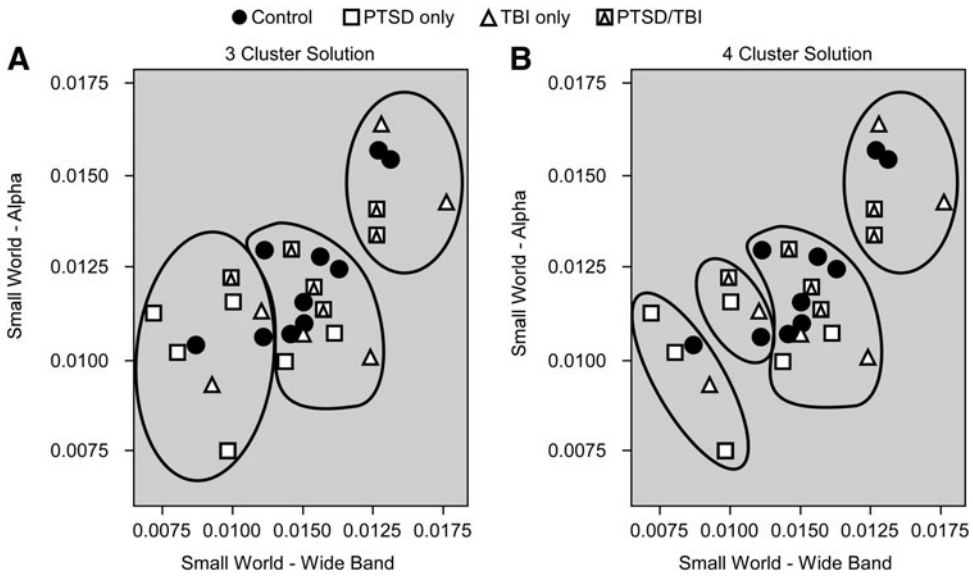

FIG. 5. Clustering analysis groupings for the three cluster solution **(A)** and four cluster solution **(B)**.

delta and beta bandwidths may be associated with specific connections within the DMN. This is consistent with resting-state studies reporting regionally distinct patterns of DMN activity occurring simultaneously across all bandwidths using EEG (Chen et al., 2008) or MEG (Hillebrand et al., 2012). Thus, while alpha may be the dominant frequency bandwidth of connectivity at rest, examining connectivity only within the alpha bandwidth may miss important connections occurring at other frequencies and artificially remove brain regions from the network. In fact, when contrasted with findings in the alpha network, the wideband network revealed *fewer* between-group differences in network metrics. This strongly suggests that a shift in connectivity from the alpha range into other parts of the frequency spectrum underlies the broad reduction in network structure found by the alpha network analysis. This hypothesis is supported by the finding of a higher percentage of connections in the Theta bandwidth in participants with mTBI-only and PTSD-only. However, even within the wideband network, significant differences in small-worldness were observed, suggesting that the shift in frequency of connectivity cannot completely account for alterations in network structure. These findings further illustrate the complex and highly individual nature of network remodeling following mTBI, PTSD, and comorbid occurrences.

Limitations and future directions

Without longitudinal studies, it is impossible to determine if the differences observed in this study were the result of PTSD and mTBI history or were present in the premorbid state. Mounting evidence suggests that many differences in brain structure may actually represent risk factors for the development of PTSD rather than consequences of the disorder (Gilbertson et al., 2002; Pitman et al., 2006). However, two groups conducting studies before and following deployment or combat exposure demonstrated changes in brain structure, function, and functional connectivity following war zone deployment (Admon et al., 2009, 2013a,b; van Wingen et al., 2011, 2012), although not directly due to the development of PTSD. Exploratory analyses to evaluate the robustness of our results demonstrate the level of heterogeneity present in the data. While trends toward clustering are present, the clinical groups do not group neatly together. It is possible this is due to variance in the effect of PTSD on functional networks or interactions between these effects and other variables not captured in the present analysis. Alternatively, the differences in network factors might represent premorbid risk factors for the development of PTSD. Heterogeneity may then be a result of these risk factors being present in undiagnosed individuals who have not experienced a sufficiently traumatic event. The

Table 4. Results of Discriminant Function Analysis of Three and Four Group Hierarchical Clustering Solutions and Clinical Diagnoses

Grouping	*Eigenvalue*	*Canonical correlation*	*Wilks lambda*	*Chi-square*	p
Three cluster					
Function 1	7.34	0.938	0.098	56.98	0.001
Function 2	0.228	0.431	0.814	5.03	0.025
Four cluster					
Function 1	15.79	0.970	0.05	72.75	0.001
Function 2	0.24	0.436	0.810	5.06	0.08
Clinical					
Function 1	0.354	0.511	0.694	8.76	0.187
Function 2	0.064	0.245	0.940	1.49	0.475

majority of participants with PTSD were taking psychiatric medications. While current findings are mixed regarding the impact of such medication on the study of PTSD (Lanius et al., 2010b), there are no studies investigating the impact on network metrics, making this a target for future investigation. Finally, larger sample sizes would increase reliability and enhance replicability. The current results did not survive FDR correction for multiple comparisons. Given the presence of moderate-to-large effect sizes, this is likely a direct result of the small sample size. However, the findings were similar across both analytic approaches, demonstrating promising reliability in the results. The smaller sample size of the current study may limit the reliability of effect sizes and the generalizability of the findings to the larger OEF/OIF/OND veteran population.

Conclusions

Applying graph-based network analysis to resting-state MEG data, this study demonstrated effects of PTSD and mTBI history on whole-brain resting-state network structure in the context of increased connectivity in the theta bandwidth. The shift in frequency of connectivity was associated with contrasting changes in network structure: increasing order and connectivity associated with mTBI history and decreasing order and connectivity in participants diagnosed with PTSD. These findings underscore the complexity of examining functional connectivity using frequency-based methods, such as the wPLI and the effect that network construction methods may have on outcomes. Simultaneously, the findings highlight the ability of graph-based network analysis to differentiate two highly comorbid disorders and provide insights not possible with other analytic techniques.

Acknowledgments

This research is supported by funding from the W.G. (Bill) Hefner Veterans Affairs Medical Center, the Wake Forest School of Medicine Translational Science Institute, and the Mid-Atlantic Mental Illness Research Education and Clinical Center (MIRECC); as well as the resources of the Department of Veterans Affairs Office of Academic Affiliations Advanced Fellowship Program in Mental Illness Research and Treatment, and the Wake Forest School of Medicine Department of Neurology and Center for Biomolecular Imaging. D.W.G. was supported by the National Institutes of Health grant R01AA016852.

Disclaimers

The views expressed in this article are those of the authors and do not necessarily reflect the position or policy of the Department of Veterans Affairs, the Department of Defense, or the U.S. government.

Author Disclosure Statement

No competing financial interests exist.

References

Admon R, Leykin D, Lubin G, Engert V, Andrews J, Pruessner J, Hendler T. 2013a. Stress-induced reduction in hippocampal volume and connectivity with the ventromedial prefrontal cortex are related to maladaptive responses to stressful military service. Hum Brain Mapp 34:2808–2816.

Admon R, Lubin G, Rosenblatt JD, Stern O, Kahn I, Assaf M, Hendler T. 2013b. Imbalanced neural responsivity to risk and reward indicates stress vulnerability in humans. Cereb Cortex 23:28–35.

Admon R, Lubin G, Stern O, Rosenberg K, Sela L, Ben-Ami H, Hendler T. 2009. Human vulnerability to stress depends on amygdala's predisposition and hippocampal plasticity. Proc Natl Acad Sci U S A 106:14120–14125.

American Psychiatric Association. 2000. *Diagnostic and Statistical Manual of Mental Disorders, Fourth Edition (DSM-IV-TR), ed*. Washington, DC: American Psychiatric Publishing.

Beal DS, Cheyne DO, Gracco VL, Quraan MA, Taylor MJ, De Nil LF. 2010. Auditory evoked fields to vocalization during passive listening and active generation in adults who stutter. Neuroimage 52:1645–1653.

Blondel VD, Guillaume J-L, Lambiotte R, Lefebvre E. 2008. Fast unfolding of communities in large networks. J Stat. Mech. 2008: P10008.

Bluhm RL, Williamson PC, Osuch EA, Frewen PA, Stevens TK, Boksman K, et al. 2009. Alterations in default network connectivity in posttraumatic stress disorder related to early-life trauma. J Psychiatry Neurosci 34:187–194.

Bosma I, Reijneveld JC, Klein M, Douw L, van Dijk BW, Heimans JJ, Stam CJ. 2009. Disturbed functional brain networks and neurocognitive function in low-grade glioma patients: a graph theoretical analysis of resting-state MEG. Nonlinear Biomed Phys 3:9.

Bullmore E, Sporns O. 2009. Complex brain networks: graph theoretical analysis of structural and functional systesm. Nat Rev Neurosci 10:186–198.

Chen A, Etkin A. 2013. Hippocampal network connectivity and activation differentiates post-traumatic stress disorder for generalized anxiety disorder. Neuropsychopharmacology 38:1889–1898.

Chen AC, Feng W, Zhao H, Yin Y, Wang P. 2008. EEG default mode network in the human brain: spectral regional field powers. Neuroimage 41:561–574.

Cheyne D, Bostan AC, Gaetz W, Pang EW. 2007. Event-related beamforming: a robust method for presurgical functional mapping using MEG. Clin Neurophysiol 118:1691–1704.

Colizza V, Flammini A, Serrano MA, Vespignani A. 2006. Detecting rich-club ordering in complex networks. Nat Phys 2:110–115.

Cornwell BR, Arkin N, Overstreet C, Carver FW, Grillon C. 2012. Distinct contributions of human hippocampal theta to spatial cognition and anxiety. Hippocampus 22:1848–1859.

Cornwell BR, Carver FW, Coppola R, Johnson L, Alvarez R, Grillon C. 2008. Evoked amygdala responses to negative faces revealed by adaptive MEG beamformers. Brain Res 1244:103–112.

Douw L, de Groot M, van Dellen E, Aronica E, Heimans JJ, Klein M, et al. 2013. Local MEG networks: the missing link between protein expression and epilepsy in glioma patients? Neuroimage 75:195–203.

Douw L, Schoonheim MM, Landi D, van der Meer ML, Geurts JJG, Reijneveld JC, et al. 2011. Cognition is related to resting-state small-world network topology: an magnetoencephalography study. Neuroscience 175:169–177.

Dunkley BT, Doesburg SM, Sedge PA, Grodecki RJ, Shek PN, Pang EW, Taylor MJ. 2014. Resting-state hippocampal connectivity correlates with symptom severity in post-traumatic stress disorder. Neuroimage Clin 5:377–384.

Engdahl B, Leuthold AC, Tan HR, Lewis SM, Winskowski AM, Dikel TN. Georgopoulos AP. 2010. Post-traumatic stress disorder: a right temporal lobe syndrome? J Neural Eng 7: 066005.

Etkin A, Wager TD. 2007. Functional neuroimaging of anxiety: a meta-analysis of emotional processing in PTSD, social anxiety disorder, and specific phobia. Am J Psychiat 164:1476–1488.

First MB, Spitzer RL, Gibbon M, Williams JBW. 1996. *Structured Clinical Interview for DSM-IV Axis I Disorders, Clinical Version (SCID-CV).* Washington, DC: American Psychiatric Press, Inc.

Geib BR, Stanley ML, Wing EA, Laurienti PJ, Cabeza R. 2015 Hippocampal contributions to the large-scale episodic memory network predict vivid visual memories. Cereb Cortex [DOI: 10.1093/cercor/bhv272].

Georgopoulos AP, Tan H-R-M, Lewis SM, Leuthold AC, Winskowski AM, Lynch JK, Engdahl B. 2010. They synchronous neural interactions test as a functional neuromarker for posttraumatic stress disorder (PTSD): a rodust classification method based on the bootstrap. J Neural Eng 7:16011.

Gilbertson M, Shenton ME, Ciszewski A, Kasai K, Lasko NB, Orr SP, Pitman RK. 2002. Smaller hippocampal volume predicts pathologic vulnerability to psychological trauma. Nat Neurosci 5:1242–1247.

Gilbertson MW, Paulus LA, Williston SK, Gurvits TV, Lasko NB, Pitman RK, Orr SP. 2006. Neurocognitive function in monozygotic twins discordant for combat exposure: relationship to posttraumatic stress disorder. J Abnorm Psychol 115: 484–495.

Han K, Mac Donald CL, Johnson AM, Barnes Y, Wierzechowski L, Zonies D, Oh J, et al. 2014. Disrupted modular organization of resting-state cortical functional connectivity in U.S. military personnel following concussive 'mild' blast-related traumatic brain injury. Neuroimage 84:76–96.

Hayasaka S, Laurienti PJ. 2010. Comparison of characteristics between region-and voxel-based network analyses in resting-state fMRI data. Neuroimage 50:499–508.

Hayes JP, Hayes SM, Mikedis AM. 2012. Quantitative meta-analysis of neural activity in posttraumatic stress disorder. Biol Mood Anxiety Disord 2:9.

Hillary FG, Rajtmajer SM, Roman CA, Medaglia JD, Slocomb-Dluzen JE, Calhoun VD, et al. 2014. The rich get richer: brain injury elicits hyperconnectivity in core subnetworks. PLoS One 9:e104021.

Hillebrand A, Barnes GR, Bosboom JL, Berendse HW, Stam C.J. 2012. Frequency-dependent functional connectivity within resting-state networks: an atlas-based MEG beamformer solution. Neuroimage 590:3909–3921.

Hillebrand A, Singh KD, Holliday IE, Furlong PL, Barnes GR. 2005. A new approach to neuroimaging with magentoencephalography. Hum Brain Mapp 25:199–211.

Huang MX, Mosher JC, Leahy RM. 1999. A sensor-weighted overlapping-sphere head model and exhaustive head model comparison for MEG. Phys Med Biol 44:423–440.

Hughes KC, Shin LM. 2011. Functional neuroimaging studies of post-traumatic stress disorder. Expert Rev Neurother 11:275–285.

Hung Y, Smith ML, Bayle DJ, Mills T, Cheyne D, Taylor MJ. 2010. Unattended emotional faces elicit early lateralized amygdala-frontal and fusiform activations. Neuroimage 50: 727–733.

Hung Y, Smith ML, Taylor MJ. 2012. Development of ACC-amygdala activations in processing unattended fear. Neuroimage 60:545–552.

Iraji A, Benson RR, Welch RD, O'Neil BJ, Woodard JL, Ayaz SI, et al. 2015. Resting state functional connectivity in mild traumatic brain injury at the acute stage: independent component and seed-based analyses. J Neurotrauma 32:1031–1045.

James LM, Engdahl BE, Leuthold AC, Lewis SM, Van Kampen E, Georgopoulos AP. 2012. Neural network modulation by trauma as a marker of resilience. Jama Psychiatry 70:410–418.

Jann K, Dierks T, Boesch C, Kottlow M, Strik W, Koenig T. 2009. BOLD correlates of EEG alpha phase-locking and the fMRI default mode network. Neuroimage 45:903–916.

King NS, Crawford S, Wenden FJ, Moss NEG, Wade DT. 1995. The Rivermead Post Concussion Symptoms Questionnaire: a measure of symptoms commonly experienced after head injury and its reliability. J Neurol 242:587–592.

Knyazev GG, Slobodskoj-Plusnin JY, Bocharov AV, Pylkova LV. 2011. The default mode network and EEG alpha oscillations: an independent component analysis. Brain Res 1402: 67–79.

Lanius RA, Bluhm RL, Coupland N, Hegadoren KM, Rowe B, Theberge J, et al. 2010a. Default mode network connectivity as a predictor of post-traumatic stress disorder symptom severity in acutely traumatized subjects. Acta Psychiatr Scand 121:33–40.

Lanius RA, Brewin CR, Bremner JD, Daniels JK, Friedman MJ, Liberzon I, et al. 2010b. Does neuroimaging research examining the pathophysiology of posttraumatic stress disorder require medication-free patients? J Psychiatry Neurosci 35: 80–89.

Laufs H, Holt JL, Elfont R, Krams M, Paul JS, Krakow K, Kleinschmidt A. 2006. Where the BOLD signal goes when alpha EEG leaves. Neuroimage 31:1408–1418.

Laufs H, Kleinschmidt A, Beyerle A, Eger E, Salek-Haddadi A, Preibisch C, Krakow, K. 2003. EEG-correlated fMRI of human alpha activity. Neuroimage 19:1463–1476.

Lei D, Li K, Li L, Chen F, Huang X, Lui S, et al. 2015. Disrupted functional brain connectome in patients with posttraumatic stress disorder. Radiology 276:818–827.

Luo Q, Cheng X, Holroyd T, Xu D, Carver F, Blair RJ. 2013. Theta band activity in response to emotional expressions and its relationship with gamma band activity as revealed by MEG and advanced beamformer source imaging. Front Hum Neurosci 7:940.

Luo Q, Holroyd T, Jones M, Hendler T, Blair J. 2007. Neural dynamics for facial threat processing as revealed by gamma band synchronization using MEG. Neuroimage 34:839–847.

Mayer AR, Mannell MV, Ling J, Gasparovic C, Yeo RA. 2011. Functional connectivity in mild traumatic brain injury. Hum Brain Mapp 32:1825–1835.

Menon DK, Schwab K, Wright DW, Maas AI. 2010. Position statement: definition of traumatic brain injury. Arch Phys Med Rehabil 91:1637–1640.

Messe A, Caplain S, Pelegrini-Issac M, Blancho S, Levy R, Aghakhani N, et al. 2013. Specific and evolving resting-state network alterations in post-concussion syndrome following mild traumatic brain injury. PLoS One 8:e65470.

Moses SN, Ryan JD, Bardouille T, Kovacevic N, Hanlon FM, McIntosh AR. 2009. Semantic information alters neural activation during transverse patterning performance. Neuroimage 46:863–873.

Neuner I, Arrubla J, Werner CJ, Hitz K, Boers F, Kawohl W, Shah NJ. 2014. The default mode network and EEG regional spectral power: a simultaneous fMRI-EEG study. PLoS One 9:e88214.

Niogi SN, Mukherjee P. 2010. Diffusion tensor imaging of mild traumatic brain injury. J Head Trauma Rehabil 25:241–255.

Palacios EM, Sala-Llonch R, Junque C, Roig T, Tormos JM, Bargallo N, Vendrell P. 2013. Resting-state functional magnetic resonance imaging activity and connectivity and cognitive outcome in traumatic brain injury. JAMA Neurol 70: 845–851.

Patel R, Spreng R, Shin L, Girard T. 2012. Neurocircuitry models of posttraumatic stress disorder and beyond: a meta-analysis of functional neuroimaging studies. Neurosci Biobehav Rev 36:2130–2142.

Pitman RK, Gilbertson MW, Gurvits TV, May FS, Lasko NB, Metzger LJ, et al. 2006. Clarifying the origin of biological abnormalities in PTSD through the study of identical twins discordant for combat exposure. Ann N Y Acad Sci 1071: 242–254.

Prichard D, Theiler J. 1994. Generating surrogate data for time series with several simultaneous measures. Phys Rev Lett 73:951–954.

Quraan MA, Moses SNHung Y, Mills T, Taylor MJ. 2011. Detection and localization of hippocampal activity using beamformers with MEG: a detailed investigation using simulations and empirical data. Hum Brain Mapp 32:812–827.

Riggs L, Moses SN, Bardouille T, Herdman AT, Ross B, Ryan JD. 2009. A complementary analytic approach to examining medial temporal lobe sources using magnetoencephalography. Neuroimage 45:627–642.

Robinson SE, Vrba J, 1998. Functional neuroimaging by synthetic aperture magnetometry (SAM). In: *Biomag98, 11th International Conference on Biomagnetism*. Sendai, pp. 1–4.

Robinson SE, Vrba J. Otsubo H, Ishii R. 2002. Finding epileptic loci by nonlinear parameterization of source waveforms. In: Nowak H, Haueisein HJ, Giessler F, Huonker R (eds.) *BIOMAG: 13th International Conference on Biomagnetism*. Jena, Germany, pp. 220–222.

Rubinov M, Sporns O. 2010. Complex network measures of brain connectivity: uses and interpretations. Neuroimage 52:1059–1069.

Schedlbauer AM, Copara MS, Watrous AJ, Ekstrom A.D. 2014 Multiple interacting brain areas underlie successful spatiotemporal memory retrieval in humans. Sci Rep 4:6431.

Seidman SB. 1983. Network structure and minimum degree. Soc Netw 5, 269–287.

Spielberg JM, McGlinchey RE, Milberg WP, Salat DH. 2015. Brain network disturbance related to posttraumatic stress and traumatic brain injury in veterans. Biol Psychiatry 78:210–216.

Sripada R, King A, Welsh R, Garfinkel S, Wang X, Sripada C, Liberzon I. 2012. Neural dysregulation in posttraumatic stress disorder: evidence for disrupted equilibrium between salience and default mode brain networks. Psychosom Med 74:904–911.

Stam CJ, Reijneveld JC. 2007. Graph theoretical analysis of complex networks in the brain. Nonlinear Biomed Phys 1:3.

Stam CJ, van Straaten ECW. 2012. The organization of physiological brain networks. Clin Neurophysiol 123:1067–1087.

Stapleton-Kotloski JR, Kotloski RJ, Boggs JA, Popli G, O'Donovan CA, Couture DE, et al. 2014. Localization of interictal epileptiform activity using magnetoencephalography with synthetic aperture magnetometry in patients with a vagus nerve stimulator. Front Neurol 5:244.

Tarapore PE, Findlay AM, Lahue SC, Lee H, Honma SM, Mizuiri D, et al. 2013. Resting state magnetoencephalography functional connectivity in traumatic brain injury. J Neurosurg 118:1306–1316.

Toppi J, De Vico Fallani F, Vecchiato G, Maglione AG, Cincotti F, Mattia D, et al. 2012. How the statistical validation of functional connectivity patterns can prevent erroneous definition of small-world properties of a brain connectivity network. Comput Math Methods Med 2012:130985.

van Wingen G, Geuze E, Caan M, Kozicz T, Olabarriaga S, Denys D, et al. 2012. Persistent and reversible consequences of combat stress on the mesofrontal circuit and cognition. Proc Natl Acad Sci U S A 109:15508–15513.

van Wingen G, Geuze E, Vermetten E, Fernandez, G. 2011. Perceived threat predicts the neural sequelae of combat stress. Mol Psychiatry 16:664–671.

Vinck M, Oostenveld R, van Wingerden M, Battaglia FC, Pennartz CMA. 2011. An improved index of phase-synchronization for electrophysiological data in the presence of volume-conduction, noise and sample-size bias. Neuroimage 55:1548–1565.

Watts DJ, Strogatz SH. 1998. Collective dynamics of ''small-world'' networks. Nature 393:440–442.

Weathers F, Litz B, Herman D, Huska J, Keane T. 1993. The PTSD checklist (PCL) reliability, validity, and diagnostic utility. Presented at the Annual Convention of the International Society for Traumatic Stress Studies, San Antonio.

Zalesky A, Fornito A, Bullmore ET. 2010. Network-based statistic: identifying differences in brain networks. Neuroimage 53:1197–1207.

Zhou Y, Wang Z, Qin LD, Wan JQ, Sun YW, Su SS, et al. 2012. Early altered resting-state functional connectivity predicts the severity of post-traumatic stress disorder symptoms in acutely traumatized subjects. PLoS One 7:e46833.

Address correspondence to:
Jared A. Rowland
Research and Academic Affairs Service Line
W.G. (Bill) Hefner VA Medical Center
1601 Brenner Avenue 11M-2
Salisbury, NC 28144

E-mail: jared.rowland@va.gov